

## Direct Electrochemistry of Catalase in Multiwall Carbon Nanotube/dodecyl Trimethylammonium Bromide Film Covered With a Layer of Nafion on a Glassy Carbon Electrode

Sedigheh Hashemnia\*, Shima Khayatzadeh, Ali Akbar Moosavi-Movahedi, Hedayatollah Ghourchian

Persian Gulf University, Bushehr 75169, Iran

Ali Akbar Moosavi-Movahedi, Hedayatollah Ghourchian

Institute of Biochemistry and Biophysics, University of Tehran, Tehran, Iran

\*E-mail: [shashemnia@pgu.ac.ir](mailto:shashemnia@pgu.ac.ir)

Received: 24 September 2010 / Accepted: 22 January 2011 / Published: 1 March 2011

---

Direct electrochemistry of catalase (Ct) was achieved by confining the protein within multiwall carbon nanotube (MWCNT)-dodecyltrimethyl ammonium bromide (DTAB) film covered with a layer of Nafion (NF) (MWCNT-DTAB-Ct/NF) on the surface of a glassy carbon electrode (GCE). The film exhibited a pair of well-defined quasi-reversible cyclic voltammetric peaks corresponding to the Fe(III)/Fe(II) redox couple in the active site of Ct with a formal potential ( $E^{\circ}$ ) = -0.279 V vs. Ag/AgCl, in 50 mM phosphate buffer solution at pH 7.0. Apparent heterogeneous electron transfer rate constant ( $10.71 \pm 0.34 \text{ s}^{-1}$ ) and charge-transfer coefficient (0.49) were estimated by Laviron's model. The process of catalytically reducing hydrogen peroxide by the MWCNT-DTAB-Ct/NF film modified electrode was also explored.

---

**Keywords:** Direct electrochemistry, Catalase, Multiwall carbon nanotube, Single- chain surfactant, Hydrogen peroxide

### 1. INTRODUCTION

In recent years, the use of electrochemical methods in studying protein and enzyme electron transfer reaction kinetics, thermodynamics, and mechanisms directly with electrodes has gained increasing attention [1-3]. Having redox enzymes directly connected to electrode made it possible to exploit the naturally high efficiency of these biological systems for electrochemical studies, biosensors, and bio-electro-analytical devices that do not use any mediators [4-7].

Ct belongs to the oxidoreductase family class and possesses a heme prosthetic group at its active site with metallic iron (Fe (III)) [8]. It exists in all almost aerobically respiring organisms and

protects cells from the toxic effects of hydrogen peroxide by catalyzing the disproportionation of hydrogen peroxide into oxygen and water without the formation of free radicals. The catalytic ability of Ct to reduce hydrogen peroxide was used in the developing of H<sub>2</sub>O<sub>2</sub> sensors [9]. One way to investigate this catalytic ability of the enzyme is to examine the direct electron transfer of Ct with electrode surface. However, studies showed that the electron transfer kinetics is very slow between the enzyme and bare electrode surface [10]. This may be due to the fact that the heme prosthetic group gets deeply buried inside the large structure of Ct. Also adsorptive denaturation of the enzyme may occur on the electrode surface. In order to achieve better electron transfer, Ct was immobilized on various modified electrode surfaces. For instance, the electrode surfaces were modified with surfactants, biopolymers, and hydrogels [11-17]. Although, these biomembrane-like films can enhance the electron transfer between the enzyme and a few electrode surfaces, most of them fail to promote the electron transfer process. This may be due to the diminished contact between the enzyme and such modified matrices. Furthermore, the matrix composition, fabrication and enzyme immobilization procedure remains rather complicated and time consuming.

To overcome these problems, the bioelectric contact between the enzyme and electrode surface was significantly improved using carbon nanotubes (CNTs) [18, 19].

CNTs are new and interesting members of carbon family, with two types of structures single-walled and multi-walled (SWCNTs and MWCNTs, respectively) [20]. They are suitable for entrapment of biological molecules and thus for fabrication of electrochemical biosensors, because of their novel properties such as high surface area, electrical conductivity, good chemical stability and extremely high mechanical strength [21-27]. However, one impediment for the potential applications of CNTs is their insolubility in most solvents, especially in water [28, 29]. But it was reported that the solubility of CNTs can be improved using polymeric chain and surfactant molecules [19, 29-34].

Surfactants are a type of amphiphilic molecules with a polar head at one end and a long hydrophobic tail at the other. They can spontaneously be adsorbed on the interfaces of two phases with different polarities and formed stable films. Surfactants usually used in these films are water-insoluble, with two long hydrocarbon chains; examples being didodecyl dimethyl ammonium bromide (DDAB), dimyristoyl-phosphatidyl-phosphate (DMPC) and dihexadecyl phosphate (DHP). These films enable detailed studies protein electron transfer and catalysis in biomembrane-like environments. Although, surfactants with two hydrophobic tails were extensively used to investigate direct electron transfer of redox proteins [19, 35, 36], few works were devoted to establishing the effect of soluble single-chain surfactants such as DTAB on electrochemical behavior of the proteins [37].

Given the ability of surfactants to inhibit adsorptive denaturation of proteins on electrode surface and to disperse CNTs as individual tubes in media, we immobilized MWCNT-DTAB-Ct/NF film on a GCE to investigate the direct electrochemistry of Ct and its catalytic activity toward hydrogen peroxide. The kinetic parameters and influence of pH were also studied based on voltammetric data. To the best of our knowledge up to date, no attempts were made to investigate electron transfer of Ct on a GCE in the presence of single-chain surfactants such as DTAB. Prakash *et al* recently studied the direct electrochemistry of Ct in the presence of DDAB as a two chain surfactant [19]. However, due to the water-insolubility of DDAB, the relationship between structure and electrochemical behavior of the protein, which is important in studying the physico-chemical

properties of proteins, still remained unexplored. The present study endeavors to investigate the relationship using DTAB as a soluble surfactant.

## 2. EXPERIMENTAL

### 2.1. Reagents

Bovine liver catalase (EC 1.11.1.6) and DTAB were purchased from Sigma-Aldrich without further purification. MWCNTs with diam. 110-170 nm, length 5-9  $\mu\text{m}$  was obtained from Aldrich. Perfluorinated ion-exchange resin (Nafion, 5% in ethanol) was obtained from Aldrich and hydrogen peroxide (30%) was purchased from Merck.

### 2.2. Apparatus

A Metrohm electroanalyzer Model 797 VA was used for voltammetric measurements. A conventional three-electrode cell was used with an Ag/AgCl electrode, a platinum rod and a GCE (diameter 2 mm) as reference, counter, and working electrode respectively. Scanning electron microscopy (SEM) images of the immobilized films on GCE were obtained with a ZIESS EM 902A scanning electron microscope. For each SEM image, the electrode tip was detached from the electrode body and coated with a thin layer of gold.

A Perkin-Elmer Lambda 25 spectrophotometer equipped with a water bath ( $\pm 0.5$  °C) was used for determination of Ct concentration as well as for recording spectra of native Ct and DTAB/Ct mixture.

We applied a circular dichroism (CD) spectrometer model 215 (Aviv Instruments INC.) for recording far-UV CD spectra of 0.2 mg/ml of the native and DTAB/Ct mixture in 50 mM phosphate buffer in the range of 190–260 nm with a spectral resolution of 1 nm. The scan speed was 20 nm/min and the response time was 0.3330 sec with a bandwidth of 1 nm. Quartz cells with an optical path of 0.1 cm were used and all measurements were done at 25 °C. The far-UV CD spectra were analyzed for the secondary structure contents of the native Ct and DTAB/Ct mixture using a cdnn program version 2 (<http://bioinformatik.biochemtech.uni-halle.de/cdnn>).

### 2.3. The working electrode Preparation

Before each experiment, the GCE was polished sequentially with 0.06  $\mu\text{m}$  alumina suspension and then on a filter paper. Thereafter, it was rinsed with doubly distilled water and sonicated with absolute ethanol and doubly distilled water for about 2 min, respectively.

MWCNT (1mg) was dispersed in 1 mL aqueous solution of DTAB (80 mM) with the aid of ultrasonication to give a 1-mg/mL stable black MWCNT suspension. MWCNT suspension (5  $\mu\text{L}$ ) was mixed with 15  $\mu\text{L}$  Ct solution (13  $\mu\text{M}$  in phosphate buffer, pH 7.0) thoroughly. Then 10  $\mu\text{L}$  of the mixture was cast onto the surface of the GCE. Afterwards, 4  $\mu\text{L}$  of 5% NF was spread onto the

MWCNT-DTAB-Ct coated electrode (MWCNTs-DTAB-Ct/NF). Finally, it was allowed to dry at room temperature for 3 h. For comparative purposes, DTAB and Ct mixtures of different ratios were prepared. All the above prepared solutions and film modified electrodes were stored at 4 °C when not in use. NF is a perfluorosulfonate ionomer that contains less than 15% ionizable sulfonate groups per monomer unit and has hydrophobic perfluoro-poly-ether chains which can bind to hydrophobic moiety of surfactant-protein complex. Incorporating the macromolecules into NF film is revealed to improve their permeability and stability [38-40].

### 3. RESULTS AND DISCUSSION

#### 3.1. Characterization of Ct in the presence of DTAB

It is well known that ionic surfactants can interact very strongly with oppositely charged globular proteins [41, 42]. At pH 7.0, DTAB and Ct possess positive and negative surface charges respectively. Then, the localized electrostatic attraction between the negatively charged Asp and Glu groups of the protein and positively charged DTAB molecules could be the main driving force for the DTAB-Ct interaction. In order to investigate the electrochemical behavior of Ct in the presence of DTAB, it is necessary that the DTAB-Ct interaction neither destroy the structure nor change the conformation of the protein heme pocket. In order to confirm this, we used UV-vis and CD spectroscopy as conventional techniques for characterizing the structure of the protein in the absence and presence of DTAB.

##### 3.1.1. Absorption spectra

Visible spectroscopy is a useful conformational probe for heme proteins.

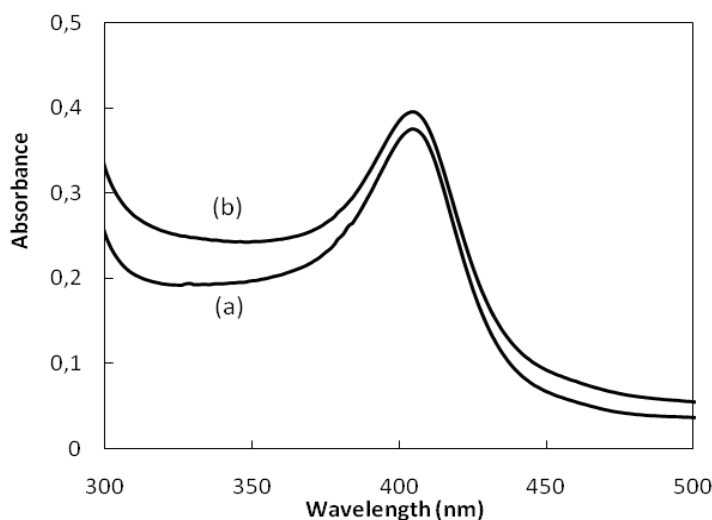


**Figure 1.** Visible absorbance spectra of the native Ct; (a) and DTAB / Ct (1900/1); (b).

The position of the Soret absorption band of heme prosthetic group may provide information about possible denaturation of heme proteins, especially conformational change about the heme pocket [43, 44]. In the present study the ratio of DTAB to Ct was the same for both UV-vis spectroscopic and electrochemical experiments. As can be seen in Fig. 1 the native Ct gives a Soret absorption maximum at 405 nm. At DTAB to Ct ratio of (1900/1) a slight enhancement is observed in Soret absorption (from 0.434 to 0.464) without any shift in wavelength maximum ( $\lambda_{\max}$ ) of absorption compared to native enzyme, indicating that no considerable change in the interaction of the heme group with the protein moiety occurs in the presence of DTAB.

### 3.1.2. Circular dichroism (CD) results

CD measurement provides an excellent means of monitoring the interaction between protein and other molecules [45]. In order to determine the effect of DTAB on the protein structure at the secondary folding level, the CD spectra of the native Ct and DTAB / Ct (1900/1) were measured. The results showed that the far UV-CD spectra of Ct in the absence and presence of DTAB at negative extremes of about 209 and 222 nm are almost similar (Fig. 2).

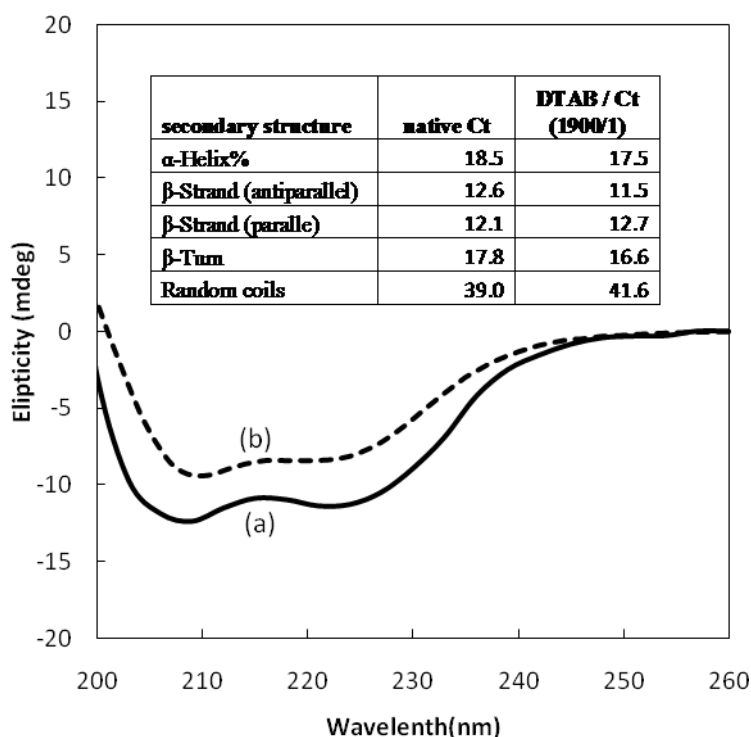


**Figure 2.** The far-UV circular dichroism spectra of the native Ct; (a) and DTAB / Ct (1900/1); (b). Inset shows the percentage of the secondary structure components for native Ct and DTAB / Ct (1900/1) obtained by cdnn program version 2.

The negative bands are accordance to the  $\pi \rightarrow \pi^*$  and  $n \rightarrow \pi^*$  amide transition of the polypeptide chain in protein respectively, and they are assigned to  $\alpha$ -helix of protein [46]. The contents of  $\alpha$ -helix,

$\beta$ -sheet,  $\beta$ -turn and random coil in each spectrum were also analyzed using the cdnn program version 2 (inset of Fig.2). Regarding the 5-10% error in software analysis, the presence of DTAB causes no significant conformational change in Ct secondary structure.

### 3.2. Morphological characterization of the MWCNTs-DTAB/NF and MWCNTs-DTAB-Ct/NF

The surface morphology of the film coated electrode was characterized by SEM. Fig. 3a reveals the presence of interconnected wires of MWCNT-DTAB covered by a layer of NF on GCE, whereas SEM image of MWCNT-DTAB-Ct/NF film (Fig. 3b) shows an uneven patterned surface. This indicates the existence of a discriminate structure morphology between MWCNTs-DTAB/NF and MWCNTs-DTAB-Ct/NF film.

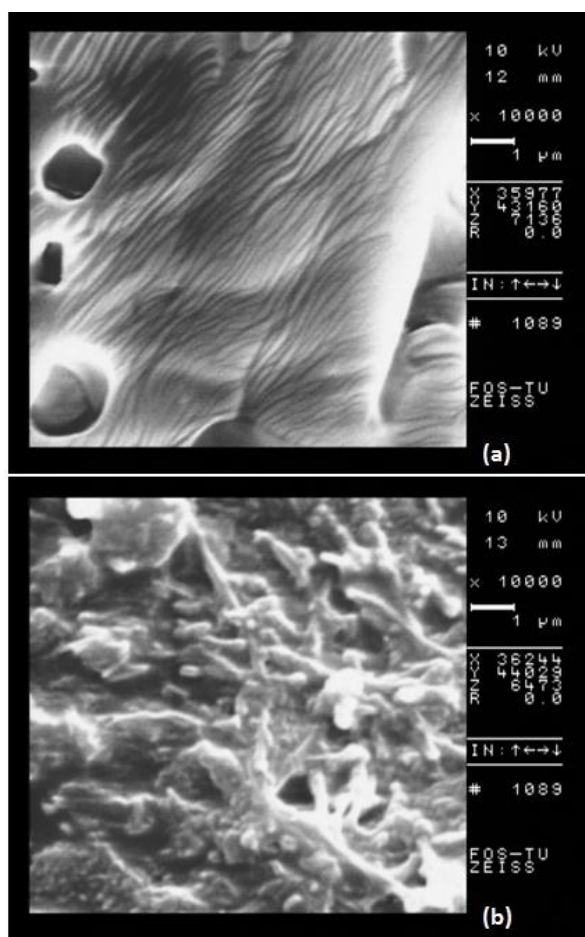
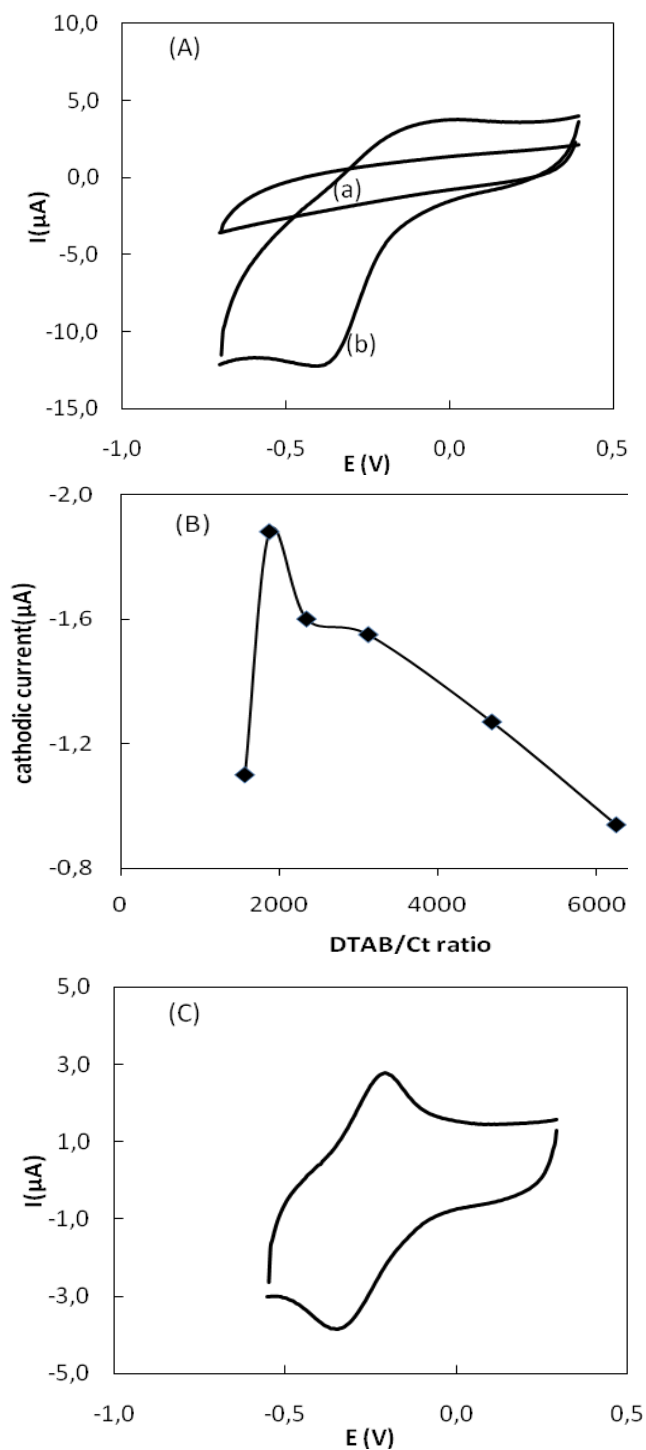


**Figure 3.** SEM images of electrode surfaces covered by: (a) MWCNT - DTAB /NF film, (b) MWCNT -DTAB- Ct/NF film.

### 3.3. Direct electrochemistry of Ct

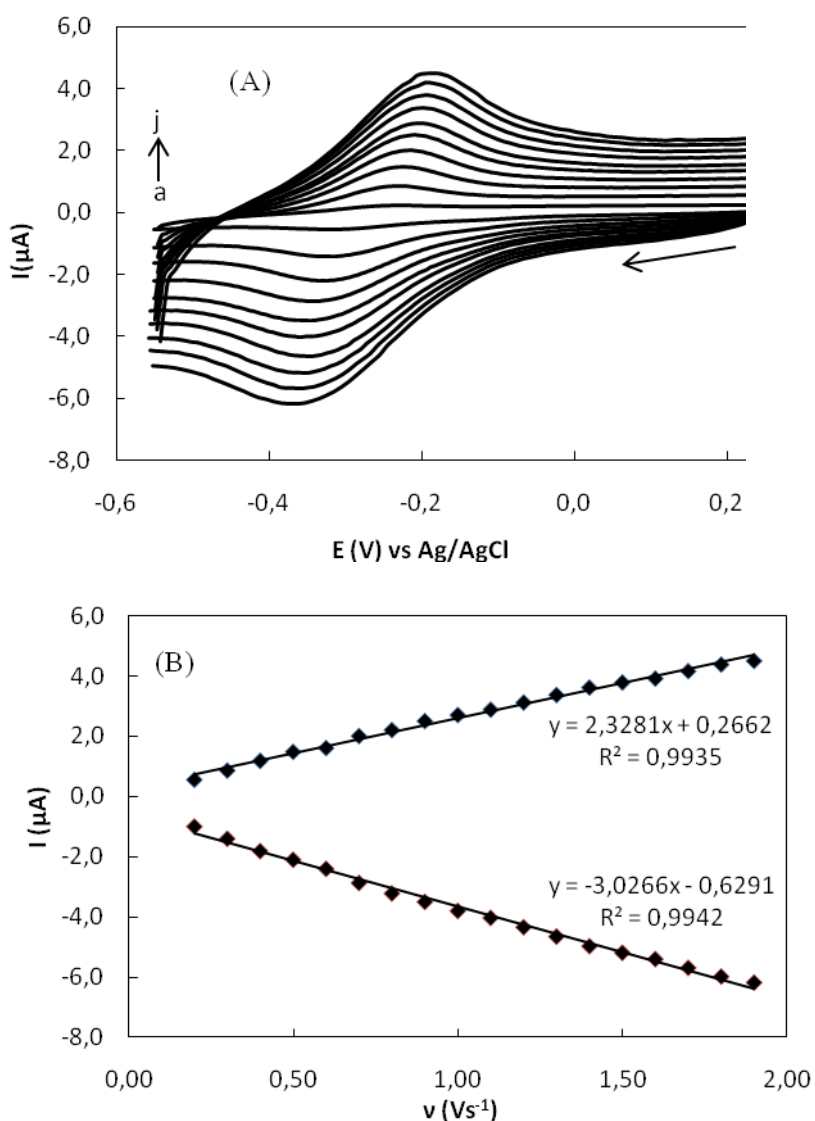
Before each experiment,  $N_2$  was purged into phosphate buffer solution for at least 20 min and a nitrogen atmosphere was maintained over the solution during the experiment. Using cyclic

voltammetry, we studied the electrochemical behavior of different film modified electrodes in 50 mM phosphate buffer, pH 7.0 (Fig. 4).



**Figure 4.** A: Cyclic voltammograms of (a) DTAB/NF film,(b) DTAB-Ct/NF film. B: Cyclic voltammogram of MWCNT-DTAB-Ct/NF film on the GCE. The experiments were carried out at scan rate of  $1 \text{ V s}^{-1}$  in 50 mM phosphate buffer pH 7.0. C: The plot of cathodic peak current vs. different ratios of DTAB/Ct present in DTAB-Ct/NF film on the GCE.

The CVs overlaid in Fig. 4A show the redox behaviors of DTAB/NF film (curve a) and DTAB-Ct/NF film (curve b) on the GCE at scan rate of  $1 \text{ V s}^{-1}$ . The DTAB/NF film on GCE exhibits no essential voltammetric response, while an irreversible reduction peak is observed at about  $-0.380 \text{ V}$  vs. Ag/AgCl for the DTAB-Ct/NF film. Fig. 4B shows the dependence of cathodic peak currents with DTAB/Ct ratio present in DTAB-Ct/NF film on GCE. The results show the maximum cathodic peak current attained with DTAB/Ct (1900:1) solution. Fig. 4C shows a pair of well-defined, quasi-reversible peak at formal potential ( $E^\circ$ ) =  $-0.279 \text{ V}$  vs. Ag/AgCl for MWCNT-DTAB-Ct/NF film, characteristic of Ct heme Fe(III)/Fe(II) redox couple [11-17]. Furthermore, to obtain well-defined quasi-reversible redox peak for the enzyme, MWCNT concentration was optimized to  $1 \text{ mg/mL}$  (data not shown). These optimized ratios were used in all the experiments. In addition in another experiment, the behavior of Ct and MWCNT-DTAB/NF on the electrode was examined. It also showed no voltammetric response (data not shown).



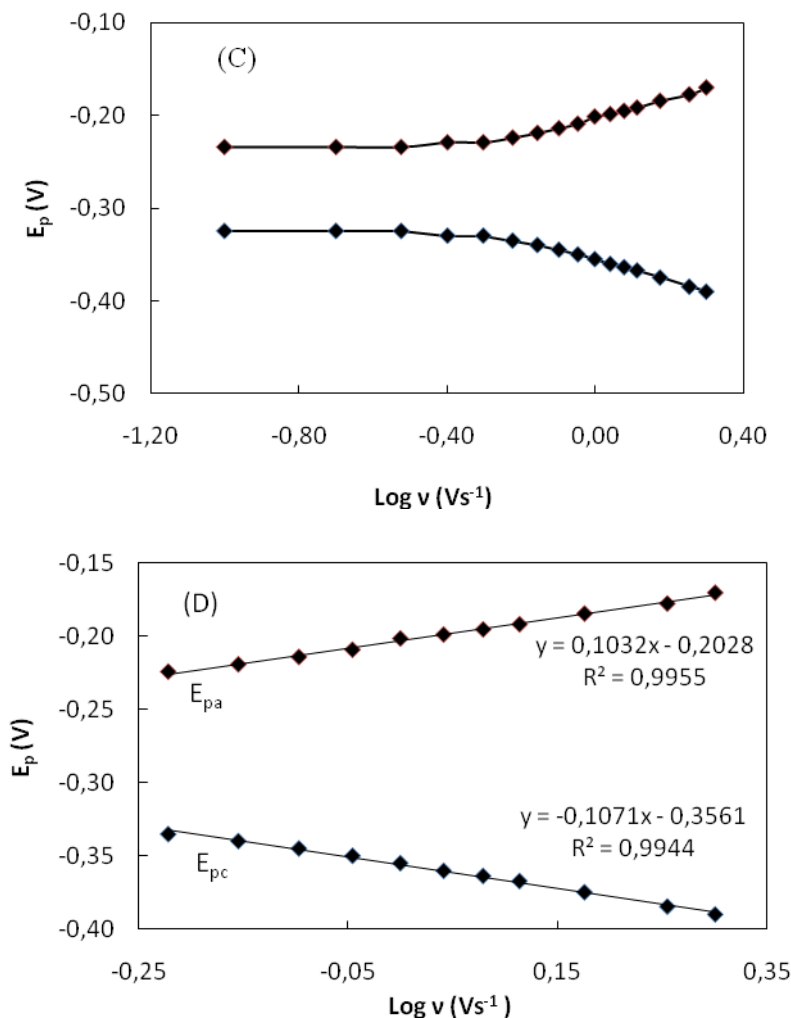


**Figure 5.** A: Cyclic voltammograms of MWCNT-DTAB-Ct/NF film modified electrode in 50 mM phosphate buffer solution, pH 7 at various scan rates of 0.1, 0.3, 0.5, 0.7, 0.9, 1.1, 1.3, 1.5, 1.7, and 1.9  $\text{Vs}^{-1}$  from a to j respectively; B: Plot of the  $I_p$  vs.  $v$ ; C: Plot of  $E_p$  vs.  $\text{Log } v$ ; D: Plot of  $E_{pc}$  and  $E_{pa}$  vs.  $\text{Log } v$ .

The formal potential  $E^{\circ'}$  (taken as the average of reduction and oxidation of peak potentials in the cyclic voltammogram) is much more positive than those reported for Ct on other modified electrodes [19, 47, 48]. As reported in the literature, the  $E^{\circ'}$  value is sensitive to the conformation of the protein. The positive shift in  $E^{\circ'}$  may be a result of the change in Ct environment in MWCNT and DTAB.

It is noteworthy that, the surface activity of the surfactant micelles might help in binding of the protein-surfactant complex to the electrode to promote electrochemical response [49]. Furthermore, CNTs are insoluble in aqueous solutions [28, 29], however, their solubility can be improved by surfactant molecules [29, 31, 34, 50]. When CNTs are dispersed by sonication in a buffer solution containing DTAB, the DTAB molecules are adsorbed onto their surfaces. The adsorption of DTAB molecules on the surfaces of CNTs can result in a distribution of positive charges that prevent the CNTs aggregation. Such an improvement of CNTs solubility in surfactant solution can be clearly seen

with the naked eye. The suspension of CNTs in DTAB solution showed to be stable for a long time (at least two weeks).

We investigated the scan rate effect to obtain the kinetic parameters of the immobilized enzyme on the GCE (Fig. 5A). A linear dependence of cathodic and anodic peak current versus scan rate was observed (Fig. 5B), indicating the electrochemical behavior of MWCNT-DTAB-Ct/NF film modified GCE. The amount of electroactive enzyme on the electrode surface can be estimated from the slope of peak currents plotted versus scan rate by the following equation [51]:

$$I_p = \frac{n^2 F^2 \nu A \Gamma}{4RT} \quad (1)$$

Where  $\nu$  is the sweep rate,  $\Gamma$  ( $\text{mol cm}^{-2}$ ) is the amount of adsorbed Ct,  $A$  ( $\text{cm}^2$ ) is the electrode surface area,  $R$ ,  $T$ , and  $F$  have their usual meanings ( $R=8.314 \text{ J mol}^{-1}\text{K}^{-1}$ ,  $T=298 \text{ K}$ ,  $F=96485 \text{ C mol}^{-1}$ ). Assuming a one-electron reaction, the amount of electroactive protein molecules is estimated to be  $2.6 \times 10^{-11} \text{ mol cm}^{-2}$ . This value is only 3.3% of the total amount of Ct deposited on the electrode surface. The relative amount of electroactive proteins on the electrode surface is always low for all heme proteins [52]. This may suggest that only those proteins in the inner layers of the film close to the electrode and with a suitable orientation can exchange electrons with the electrode surface.

An estimation of the kinetic parameters  $\alpha$  (charge transfer coefficient) and  $k_s$  (heterogeneous transfer rate constant) was carried out using the Laviron's model (for  $n\Delta E_p > 0.200 \text{ V}$ , Eq. 2) [53].

$$\log k_s = \alpha \log(1 - \alpha) + (1 - \alpha) \log \alpha - \log \frac{RT}{nF\nu} - \frac{\alpha(1 - \alpha)nF\Delta E_p}{2.3RT} \quad (2)$$

Here,  $n$  is the number of electrons transferred in the rate-determining reaction ( $n=1$ ),  $\Delta E_p$  is the peak potential separation, and  $\nu$  is the scan rate,  $R$ ,  $T$ , and  $F$  have their usual meanings.  $\alpha$  can be calculated using the plot of peak potentials vs. logarithm of scan rates ( $\log \nu$ ) (Fig. 5C). As seen in Fig. 5D, the plot of  $E_p$  vs.  $\log \nu$  at scan rates above  $0.6 \text{ Vs}^{-1}$ , yields two straight lines with slopes of  $-2.3RT/\alpha nF$  and  $2.3RT/(1-\alpha)nF$  for the cathodic and anodic peaks respectively. Thus, using the slopes of the mentioned plot, the average value for  $\alpha$  could be estimated to be 0.49. From the values of  $\Delta E_p$  (for scan rates  $> 1.8 \text{ Vs}^{-1}$ ), the average value of  $k_s$  was obtained to be  $10.71 \pm 0.34 \text{ s}^{-1}$ . The value of  $k_s$  being higher than those reported for heme proteins on other electrodes [52, 54], indicates that this immobilization method provides a favorable microenvironment for Ct and enhances the rate of electron transfer between the enzyme and electrode.

### 3.4. Reproducibility and stability of the MWCNT-DTAB-C/NF film

The reproducibility of the MWCNT-DTAB-Ct/NF film modified electrode response described above was examined at five electrodes prepared under the same conditions. The relative standard deviation (%RSD) was 6.8% for an average  $i_{pc}$  of  $3.48 \mu\text{A}$  at scan rate  $1 \text{ Vs}^{-1}$  in  $50 \text{ mM}$  phosphate buffer pH 7.0.

The stability of MWCNT-DTAB-Ct/NF film modified electrode was investigated by cycling the electrode potential over the range 0.3 to -0.55V. According to Fig. 6, after 100 cycles the peak potential remained nearly unchanged while the peak current reduced for 11.4%. The decrease in current is probably due to the loss of loosely attached MWCNT-DTAB-Ct from the electrode surface.

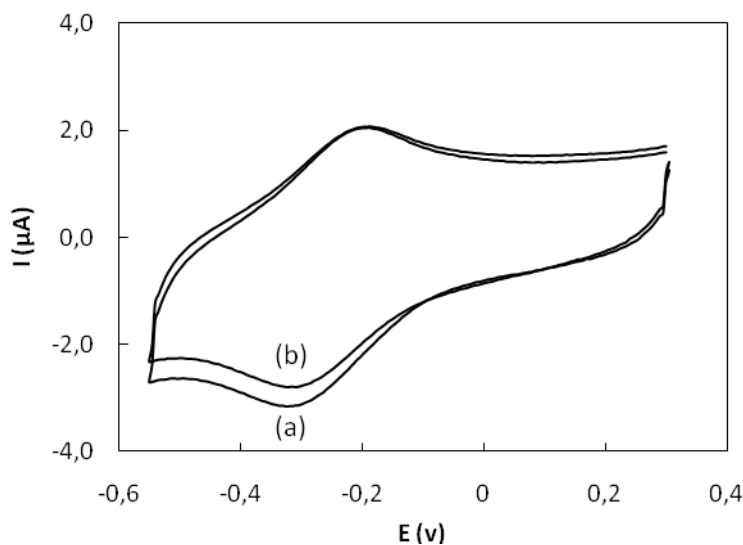


**Figure 6.** The 1<sup>st</sup> (a), and 100<sup>th</sup> (b) recorded cyclic voltammogram of MWCNT-DTAB-Ct/NF film on the GCE in 50 mM phosphate buffer solution (pH 7.0) at scan rate of 1 Vs<sup>-1</sup>.

### 3.5. Influence of pH on voltammetry

The solution pH dependence of MWCNT-DTAB-Ct/NF film modified electrode was also investigated.

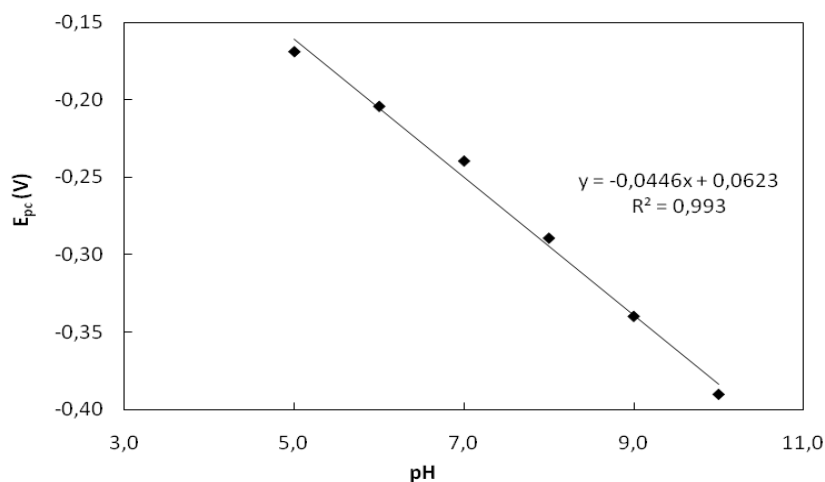


**Figure 7.** Plot of cathodic peak potential vs. pH (5-10) for the MWCNT-DTAB-Ct/NF on the GCE. Inset shows cyclic voltammograms of the film on the electrode surface in 50 mM phosphate buffer (a) pH 7.0, and (b) pH 5.0.

As can be seen in Fig. 7 within the pH range of 5-10, the reduction peak potential shifts to the cathodic direction with a slope of 0.044 V per unit of pH. It indicates that the electrode reaction is accompanied by proton transfer. The value of the slope is smaller than the theoretically expected value of 0.059 V  $\text{pH}^{-1}$  for the reaction of one electron coupled one proton. This might be due to the influence of protonation states of trans ligands of the heme iron and amino acids around the heme, or the protonation of the water molecule coordinated to the central iron [55, 56]. It is noteworthy that at pH 7.0, the Ct redox peaks were found to be best defined (inset of Fig. 7). Therefore, we fixed the solution pH at 7.0 for the investigations of the analytical performance of MWCNT-DTAB-Ct/NF film modified electrode.

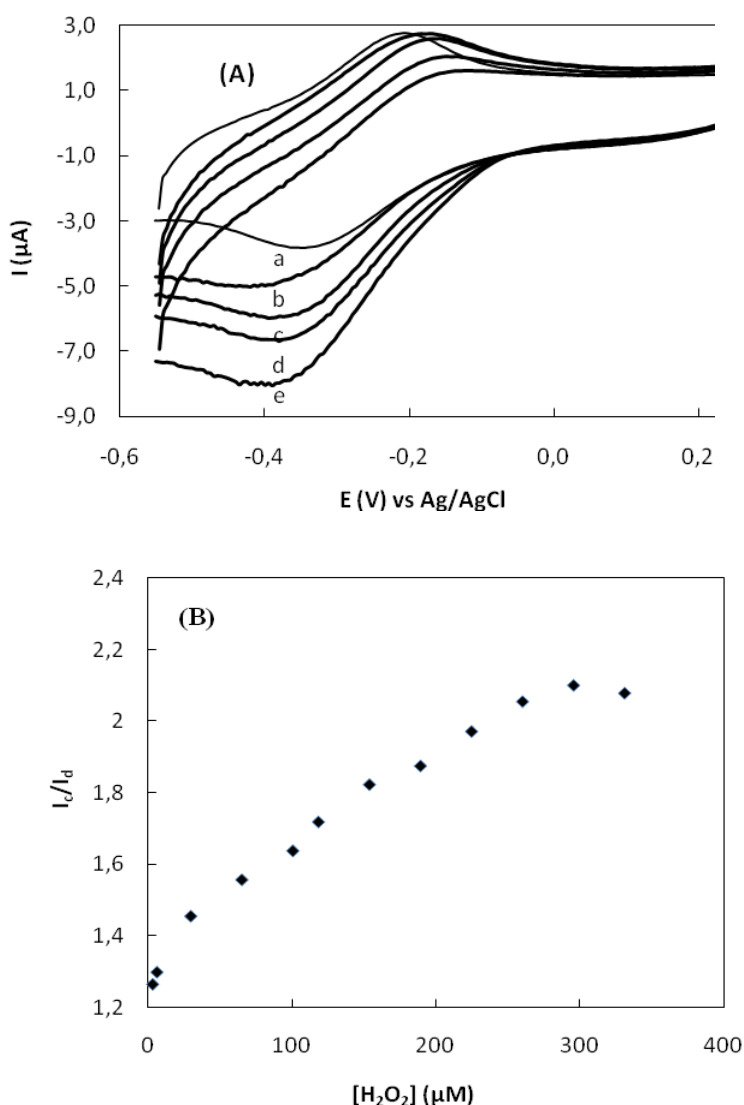
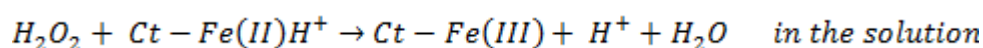
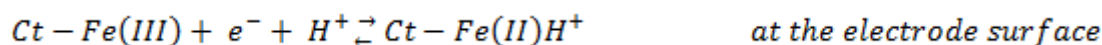


**Figure 8.** A: Cyclic voltammograms of MWCNT-DTAB-Ct/NF film on the electrode in the absence (a) and presence of 5.8  $\mu\text{M}$  (b), 65.0  $\mu\text{M}$  (c), 189.0  $\mu\text{M}$  (d), and 330  $\mu\text{M}$  (e) hydrogen peroxide. B: Catalytic efficiency changes versus the concentration of hydrogen peroxide, where  $I_c$  and  $I_d$  are cathodic peak currents in the presence and absence of hydrogen peroxide, respectively. Inset shows the calibration plot for hydrogen peroxide determination. The electrolyte solution was 50 mM phosphate buffer solution (pH 7) and scan rate was 1  $\text{Vs}^{-1}$

### 3.6. Catalytic activity of Ct

Bio-electrocatalytic reduction of hydrogen peroxide was carried out on MWCNT-DTAB-Ct/NF film modified electrode by cyclic voltammetry in 50 mM phosphate buffer solution (pH 7.0) and at scan rate of  $1\text{Vs}^{-1}$  (Fig. 8A).

By increasing the concentration of  $\text{H}_2\text{O}_2$ , an increase in the reduction peak occurred along with a decrease in the oxidation peak during the scan reversal; while in the applied potential range and in the absence of the enzyme,  $\text{H}_2\text{O}_2$  was not reduced on either bare GCE or MWCNT-DTAB/-NF film modified electrode. Thus the electrode reaction is characteristic of an  $\text{E}_r\text{C}_i'$  mechanism [51]:



Where Ct-Fe(III) and Ct-Fe(II) denote the oxidized and reduced forms of Ct, respectively. As can be seen from the suggested mechanism, once Ct-Fe(III) undergoes the electron transfer reaction with the modified electrode, Ct-Fe(II)H<sup>+</sup> can be oxidized by  $\text{H}_2\text{O}_2$  in the solution to regenerate Ct-Fe(III). The above electrode reaction slightly differs from the conventional  $\text{E}_r\text{C}_i'$  mechanism in that both Ct-Fe(III) and Ct-Fe(II)H<sup>+</sup> are surface confined.

Fig.8B shows that catalytic efficiency ( $I_c/I_d$ ) changes versus the concentration of  $\text{H}_2\text{O}_2$ , where  $I_c$  and  $I_d$  are the cathodic peak currents in the presence and absence of  $\text{H}_2\text{O}_2$ .

By increasing the concentration of  $\text{H}_2\text{O}_2$  up to about 260  $\mu\text{M}$  the catalytic efficiency is increased, then it tends to level off. A linear relationship between the catalytic efficiency and  $\text{H}_2\text{O}_2$  concentration is observed between 30 and 260  $\mu\text{M}$ . based on this, the protein film has a promising potential in fabricating an enzyme biosensor for determination of hydrogen peroxide.

## 4. CONCLUSION

MWCNT-DTAB-Ct/NF film on GCE was shown to be able to establish a direct electron transfer between the enzyme and electrode. This can be attributed to an excellent microenvironment that MWCNT- DTAB /NF provides to Ct. However, UV-vis and CD spectra suggested that the native conformation of Ct in the film was unchanged and heme active center of the protein remains intact in the presence of DTAB.

The presence of MWCNTs in the film caused the change of irreversible reduction peak of Ct in DTAB- Ct/ NF film to a pair of well-defined redox peaks. Further, the film showing a rapid response with catalytic activity towards the reduction of hydrogen peroxide reveals a new path for the development of enzyme based mediator less sensor.

## ACKNOWLEDGMENT

We gratefully acknowledge the financial support of the Research Council of Persian Gulf University. The cooperation of the electron microscope staff at College of Science, University of Tehran is also acknowledged.

## References

1. C. Leger and P. Bertrand, (2008) *Chem. Rev.*, 108 (2008) 2379.
2. F. A. Armstrong and G. S. Wilson, *Electrochim. Acta*, 45 (2000) 2623.
3. H. A. O. Hill, *Coord. Chem. Rev.*, 151 (1996) 115.
4. W. Zhang and G. Li, *Anal. Sci.*, 20 (2004) 603.
5. L. Stoica, R. Ludwig, D. Haltrich and L. Gorton, *Anal. Chem.*, 78 (2006) 393.
6. L. D. Mello and L. T. Kubota, *Talanta*, 72 (2007) 335.
7. M. Pita and E. Katz, *J. Am. Chem. Soc.*, 130 (2008) 36-.
8. P. Nicholls and G. R. Schonbaum In: Boyer P D, Lardy H, Myrback K, (Eds.), *The Enzymes*, Vol. 8, Academic Press, Orlando (1963).
9. M. Buleandra, G. L. Radu and I. Tanase, *Roum. Biotechnol. Lett.*, 5 (2000) 423.
10. M. E. Lai and A. Bergel, *Bioelectrochemistry*, 55 (2002) 157.
11. X. Chen, H. Xie, J. Kong and J. Deng, *Biosens. Bioelectron.*, 16 (2001) 115.
12. H. Huang, N. Hu, Y. Zeng and G. Zhou, *Anal. Biochem.*, 308 (2002) 141.
13. H. Y. Lu, Z. Li and N. Hu, *Biophys. Chem.*, 104 (2003) 623.
14. Y. M. Li, X.T. Chen, J. Li and H. H. Liu, *Electrochim. Acta*, 49 (2004) 3195.
15. M. Li, P. He, Y. Zhang and N. Hu, *Biochim. Biophys. Acta*, 1749 (2005) 43.
16. S. F. Wang, T. Chen, Z. L. Zhang, D. W. Pang and K. L. Wong, *Electrochem. Commun.*, 9 (2007) 1709.
17. L. Shen and N. Hu, *BBA-Bioenergetics*, 1608 (2004) 23.
18. L. Wang, J. Wang and F. Zhou, *Electroanal.*, 16 (2004) 627.
19. P. A. Prakash, U. Yogeswaran and S. M. Chen, *Talanta*, 78 (2009) 1414.
20. J. J. Gooding, *Electrochim. Acta*, 50 (2005) 3049.
21. P. M. Ajayan, *Chem. Rev.*, 99 (1999) 1787.
22. M. F. Yu, O. Lourie, M. J. Dyer, K. Moloni, T. F. Kelly and R. S. Ruoff, *Science*, 287 (2000) 637.
23. J. Wang, *Electroanal.*, 17 (2005) 7.
24. U. Yogeswaran, S. Thiagarajan and S. M. Chen, *Sensors*, 8 (2008) 7191.
25. U. Yogeswaran and S. M. Chen *Anal. Lett.*, 41(2008) 210.
26. J. N. Coleman, U. Khan, W. J. Blau and Y. K. Gunko, *Carbon*, 44 (2006) 1624.
27. A. J. Saleh Ahammad, J. J. Lee and Md. Aminur Rahman, *Sensors*, 9 (2009) 2289.
28. C. Journet, W. K. Maser, A. Loiseau, M. Lamy de la Chapelle, S. Lefrant, P. Deniard, R. Lee and J. E. Fischer, *Nature*, 388 (1997) 756.
29. A. Star, J. F. Stoddart, D. Streuerman, M. Diehl, A. Boukai, E. W. Wong, X. Yang, S. W. Chung, H. Chio and J. R. Heath, *Angew. Chem. Int. Ed.*, 40 (2001) 1721.
30. J. E. Riggs, Z. Guo, D. L. Carroll and Y. P. Sun *J. Am. Chem. Soc.*, 122 (2000) 5879.
31. J. Wang, M. Musameh and Y. Lin *J. Am. Chem. Soc.*, 125 (2003) 2408.
32. C. Richard, F. Balavoine, P. Schultz, T. W. Ebbesen and C. Mioskowski, *Science*, 300 (2003) 775.
33. M. J. O. Connell, P. Poul, L. Ericson, C. Huffman, Y. Wang, E. Haroz, C. Kuper, J. Tour, D. Ausman and R. E. Smalley, *Chem. Phys. Lett.*, 342 (2001) 265.
34. C. X. Cai and J. Chen, *Anal. Biochem.*, 325 (2004) 285-.
35. Y. Xu, C. Hu and S. Hu, *Biochemistry*, 74 (2009) 254.
36. R. Vittal, H. Gomathi and K. J. Kim, *Adv. Colloid. Interface. Sci.*, 119 (2006) 55.
37. Y. Xu, C. Hu and S. Hu, *Bioelectrochemistry*, 72 (2008)135.

38. T. Samejima and J. T. Yang, *J. Biol. Chem.*, 238 (1963) 3256.
39. E. Szajdzinska-Pietek, J. Pilar and S. Schlick, *J. Phys. Chem.*, 99 (1995) 313.
40. R. Rabago, R. D. Noble and C. A. Koval, *Chem. Mater.*, 6(1994) 947.
41. A. A. Moosavi-Movahedi,, K. Nazari and A. A. Saboury, *Colloids Surf. B: Biointerfaces*, 9 (1997): 123.
42. J. Chamani and A. A. Moosavi-Movahedi, *J. Colloid. Interface. Sci.*, 297 (2006) 561.
43. P. George and G. I. H. Hanania, *J. Biochem.*, 55 (1953) 236.
44. T. T. Herskovits and H. Jailliet, *Science*, 163(1969) 282.
45. J. Greve, M. F. Maestre, H. Moise and J. Hosoda, *Biochemistry*, 17 (1978) 887.
46. Y. P. Myer, *J. Biol. Chem.*, 243(1968) 2115.
47. H. Lu, Z. Li and N. Hu, *Biophys. Chem.*, 104 (2003) 623.
48. A. Salimi, A. Noorbakhsh and M. Ghadermarz, *Anal. Biochem.*, 344 (2005) 16.
49. K. Chattopadhyay and S. Mazumdar, *Biochemistry*, 42 (2003) 14606.
50. J. E. Riggs,, Z. Guo, D. L. Carroll and Y. P. Sun, *J. Am. Chem. Soc.*, 122 (2000) 5879.
51. A. J. Bard and L. R. Faulkner, *Electrochemical methods: fundamentals and applications*, Wiley, New York (2001).
52. S. F. Wang, T. Chen, Z. L. Zhang, X. C. Shen, Z. X. Lu, D. W. Pang and K. Y. Wong, *Langmuir*, 21(2005) 9260.
53. E. Laviron, *J. Electroanal. Chem.*, 101(1979) 19.
54. Q. Huang, Z. Lu and J. F. Rusling, *Langmuir*, 12 (1996) 5472.
55. I. Yamazaki, T. Ariaso, Y. Hayashi, H. Yamada and R. Makino, *Adv. Biophys.*, 11(1978) 249.
56. S. Hashemnia, H. Ghourchian, A. A. Moosavi-Movahedi and H. Faridnouri, *J. Appl. Electrochem.*, 39 (2009)7.